2013

Coarse-Grained Models for Momentum, Energy and Species Transport in Gas-Particle Flows

Sankaran Sundaresan
Princeton University

Stefan Radl
Gratz University of Technology

Christian C. Milioli
Princeton University

Fernando E. Milioli
Princeton University

Follow this and additional works at: http://dc.engconfintl.org/fluidization_xiv

Recommended Citation

Coarse-Grained Models for Momentum, Energy and Species Transport in Gas-Particle Flows

Sankaran Sundaresan[a], Stefan Radl[b], Christian C. Milioli[a] and Fernando E. Milioli[a]
[a]Dept. of Chemical and Biological Engineering, Princeton University, 08544
Princeton, NJ, USA; T: 1-609-258-4583; E: sundar@princeton.edu
[b]Graz University of Technology; Institute for Process and Particle Engineering,
Inffeldgasse 13/III, 8010 Graz, Austria, T: 43-316-873-30412, E: radl@tugraz.at

ABSTRACT

Coarse-grained (a.k.a. filtered) models for gas-particle flows strive to resolve coarse flow structures, while capturing the consequences of smaller scale processes through filter-size dependent closures. Through a combination of Euler-Euler and Euler-Lagrange simulations, we find that at small length scales the principal competition is between gravitational and particle phase stress, while at larger length scales it is between gravitational and particle inertia.

INTRODUCTION

Gas-particle flows in bubbling and circulating fluidized beds are inherently unstable, and they manifest fluctuations in velocities and local suspension density over a wide range of length and time scales. As in single-phase turbulent flows, it is impractical to resolve all the scales of fluctuations in process devices. Coarse-grained models for such flows strive to resolve only the coarse flow structures; the consequences of smaller scale processes appear in these models through filter-size dependent closures for the inter-phase exchange rates, effective stresses and scalar dispersion coefficients ([1],[2]). These closures have been developed in the literature by analyzing the flow structures observed in detailed simulations of fluidized systems using typical values for the properties of gases and particles. Proper adaptation of these closures to other gas-particle systems require good understanding of the characteristic scales which must be used to cast the transport problem in dimensionless form, which motivates the following simple question.

Consider fluidization of monodisperse particles (of diameter d_1 and density ρ_{s1}) by a gas (of viscosity μ_{g1} and density ρ_{g1}) in a periodically repeating domain characterized by length Δ_{d1}. Let the terminal settling velocity of this particle and the average volume fraction of particles in the domain be denoted by u_{t1} and $\langle \phi_s \rangle$, respectively. Upon fluidization, which is sustained by imposing an average pressure gradient of $\left(\rho_{s1}\phi_s + \rho_{g1}\phi_g \right)\boldsymbol{g}$, inhomogeneous structures will form and the average slip velocity u_{s1} in the statistical steady state will, in general, be different from that for the homogeneously fluidized state, namely, u_{s1}^o. Unlike u_{s1}^o, u_{s1} depends on Δ_{d1}. $u_{s1}\left(\Delta_{d1} \to 0 \right) = u_{s1}^o$; it increases monotonically with Δ_{d1} and $u_{s1}\left(\Delta_{d1} \to \infty \right) = u_{s1}^\infty$. Let us now suppose that we are given a second geometrically similar system (where all

quantities are now denoted by subscript 2) with the same $\langle \phi_s \rangle$ and are asked to identify conditions that would ensure that these two systems are *similar*.

As the flow characteristic of each system is dynamic in nature, we must be specific about the extent of similarity. For similarity at all scales, one must match all possible dimensionless groups between the two systems. Dimensional analysis leading to a list of relevant dimensionless groups in fluidization problems has been studied extensively in the literature; e.g., see ref. (3,4,5). In general, it is difficult to match all these dimensionless groups in laboratory experiments, and this has led people to investigate how one can partition these dimensionless groups into those that are critical and those which are of secondary importance; e.g., see ref. (4,5).

In the fluidization example that we posed above, as the average slip velocity is an important *macroscopic* quantity of interest, we ask how Δ_{d1} and Δ_{d2} should be related so that $u_{s1}/u_{t1} = u_{s2}/u_{t2}$. Through Euler-Lagrange simulations of fluidization in *very small periodic domains* where particle interactions are tracked (commonly known in the fluidization community as Computational Fluid Dynamics-Discrete Element Method, CFD-DEM), we have identified the scaling that very nearly achieves this similarity: $\Delta_{d1}/L_{II,1} = \Delta_{d2}/L_{II,2}$, where $L_{II} = \left(u_t^2/g \right) Fr_p^{-2/3}$. Here $Fr_p = u_t^2/gd$ is the particle Froude number. This scaling naturally arises when viscous and gravitational forces balance each other and the particle phase viscous stress is modeled using kinetic theory of granular materials.

We then examined similarity in *much larger periodic domains* via kinetic theory based two-fluid model simulations. We filtered the results in such simulations using filters of different sizes and examined how various filtered quantities should be scaled in order to best match the two fluidized beds. As explained in detail below, an *inertial* characteristic length $L_I = u_t^2/g$ emerged as an alternate, and perhaps more relevant, scale. This scaling emerges when inertial and gravitational forces balance each other.

TWO-FLUID MODEL

We begin with the widely used two-fluid model for gas-particle flows:

$$\frac{\partial}{\partial t}\left(\rho_i \phi_i \right) + \nabla \cdot \left(\rho_i \phi_i \mathbf{v}_i \right) = 0, \quad i = s, g \tag{1}$$

$$\left[\frac{\partial}{\partial t}\left(\rho_g \phi_g \mathbf{v}_g \right) + \nabla \cdot \left(\rho_g \phi_g \mathbf{v}_g \mathbf{v}_g \right) \right] = -\nabla \cdot \sigma_g - \mathbf{\Phi} + \rho_g \phi_g \mathbf{g} \tag{2}$$

$$\left[\frac{\partial}{\partial t}\left(\rho_s \phi_s \mathbf{v}_s \right) + \nabla \cdot \left(\rho_s \phi_s \mathbf{v}_s \mathbf{v}_s \right) \right] = -\nabla \cdot \sigma_s + \mathbf{\Phi} + \rho_s \phi_s \mathbf{g} \tag{3}$$

Here, the interaction force term is written as $\mathbf{\Phi} = -\phi_s \nabla \cdot \sigma_g + \beta \left(\mathbf{v}_g - \mathbf{v}_s \right)$ where β is the friction coefficient, for which the model proposed by Wen & Yu (6) is among the

most widely used. In most fluidized beds, $\rho_s \phi_s \gg \rho_g \phi_g$; so, the inertial terms on the left hand side of the particle phase momentum balance (eq. 3) are much more important than those in the gas phase momentum balance (eq. 2). Furthermore, the gas-phase deviatoric stress is of little consequence; hence $\nabla \cdot \sigma_g \approx \nabla p_g$. The particle phase stress is usually modeled using the kinetic theory of granular materials – e.g., see ref. (7,8). It is well known that in gas-fluidized beds, the gas phase pressure gradient in the vertical direction, the fluid particle-drag force and the gravitational force on the particles are all of the same order of magnitude.

We observe that the rate of dissipation of mechanical energy per unit volume in our test example scales as $\rho_s \langle \phi_s \rangle u_t g$; this represents conversion of mechanical energy to thermal energy through inelastic collisions and viscous dissipation in the gas phase. By demanding that the rate of dissipation by inelastic collisions (in the granular energy balance) scale as $\rho_s \langle \phi_s \rangle u_t g$, we find that the granular temperature $T \sim (u_t g d)^{2/3}$; it then follows that the kinetic-theory-based estimate for particle phase viscosity is: $\mu_s \sim \rho_s d (u_t g d)^{1/3}$. In contrast, phenomenological models often postulate that $\mu_s \sim \rho_s u_t d$.

One can readily ascertain through numerical simulations that in our test problem the gas and particle phase velocities scale with the terminal settling velocity. Thus, proper scaling of eqs. (1)-(3) should employ particle density and terminal settling velocity as core variables, leaving us the task of identifying the characteristic length, for which we have several choices:

1. $L_I = u_t^2 / g$ to balance the inertial and gravitational terms in eq. (2);

2. $L_{II} = (u_t^2 / g) Fr_p^{-2/3}$ to balance the viscous and gravitational terms using the kinetic theory based scaling for viscosity;

3. $L_{III} = (u_t^2 / g) Fr_p^{-1/2}$ to balance the viscous and gravitational terms using the phenomenological scaling for viscosity;

4. $L_{IV} = (u_t^2 / g) Fr_p^{-1} = d$ to balance the viscous and inertial terms using the phenomenological scaling for viscosity; and

5. $L_V = (u_t^2 / g) Fr_p^{-4/3}$ to balance the viscous and inertial terms using the kinetic theory based scaling for viscosity.

These can be written compactly as $L = (u_t^2 / g) Fr_p^n$, with optimal choice of the exponent *n* remaining to be found.

CFD-DEM APPROACH

In this approach (9), we solve the Newton's equations of motion for all the particles instead of the *continuum* particle phase continuity and momentum balances presented above. The particles are assumed to be frictional, inelastic spheres,

interacting with each other through a linear spring-dashpot model with frictional slider ("soft sphere approach"). Details are omitted for the sake of brevity.

NUMERICAL SIMULATIONS AND RESULTS

CFD-DEM Simulations

The parameters used in the base case simulations are as follows: d = 75 μm; gas and particle densities are 1.3 and 1500 kg/m^3; gas viscosity = 1.8x10^{-5} Pa.s. The corresponding terminal settling velocity = 0.219 m/s. The particle Froude number and Reynolds number (based on terminal velocity) are 65 and 1.18, respectively. Simulations were performed in a $\left(\Delta_d, \Delta_d, 4\Delta_d\right)$ periodic domain, with Δ_d =4mm and various $\langle \phi_s \rangle$ between 0.02 and 0.25 (typical for CFB risers), but we present below only the time-averaged value of the scaled domain-average slip velocity in the statistical steady state for $\langle \phi_s \rangle$ = 0.05. The simulation domain was discretized into 16x16x64 fluid grids for this base case. The DEM model parameters were assigned typical values, but they did not have any significant effect on the slip velocity and so are not listed.

We then carried out simulations for particles of several different diameters, while fixing all the other parameters. Clearly, this is one way of changing the
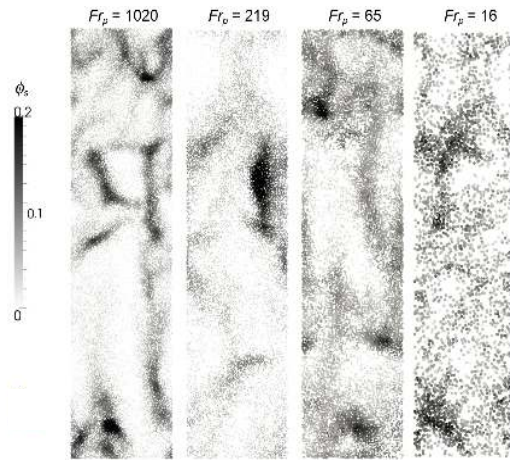

Figure 1: Snapshots of particle distribution for various Fr_p.
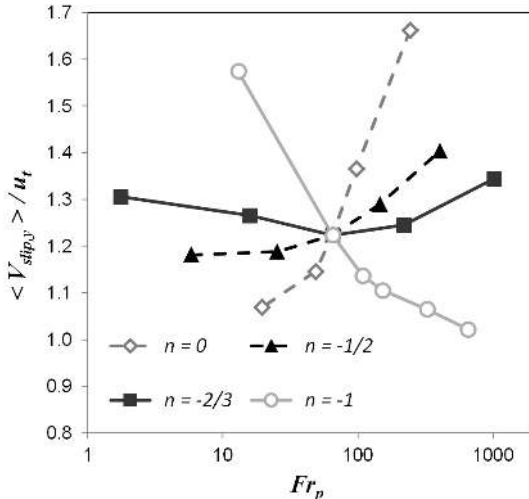

Figure 2: Summary of domain-average slip velocities.

particle Froude and Reynolds numbers. The domain size was scaled using various choices for the reference length described above. The fluid grid resolution was maintained at 16x16x64, which is equivalent to saying that the same reference length was used to scale both the domain and fluid cell lengths. The scaled domain-average slip velocity was computed in each case.

Figure 1 shows snapshots of particle volume distributions in a thin vertical slice (~7 particle diameters thick) for different Froude numbers (with $\langle \phi_s \rangle$ = 0.05) in simulations employing L_{II} as the characteristic length. Analogous results are obtained for other characteristic lengths as well. The formation of such structures lowers gas-particle interaction and hence to gas flow rate needed to support the weight of the particles is

larger than what one would need in a homogeneous suspension. Figure 2 shows the scaled domain-average slip velocity corresponding to several different choices of characteristic lengths and $\langle \phi_s \rangle$ = 0.05. It is readily clear that the best results are obtained for n = -2/3. This suggests that at such small scales (only of the order of a few tens of particle diameters, as can be discerned by the size of the simulation domain), the appropriate length scale is set by the competition between gravity and effective particle phase deviatoric stress arising through particle-particle interaction. Note that the Reynolds number is different in the various simulations, but was not taken into consideration in the scaling analysis. It appears in the expression for the friction coefficient; yet, it apparently plays only a secondary role.

Two-fluid Model Simulations

Using MFIX (10) as the simulation platform, transient simulations of a kinetic theory based two-fluid model (7) were also performed for the base case mentioned above in a large two-dimensional square periodic domain (16cm x 16cm) with a grid resolution of 0.125cm x 0.125cm. The results in the statistical steady state of such simulations were filtered using filters of different sizes, as described in detail elsewhere (11). Simulations were done for several different filter sizes, filtered volume fraction and $\langle \phi_s \rangle$, but for the sake of brevity we present, as a representative case, only the results obtained for a filter size of 4 cm (for the base case) and filtered particle volume fraction of 0.15 obtained from simulations with $\langle \phi_s \rangle$ = 0.15.
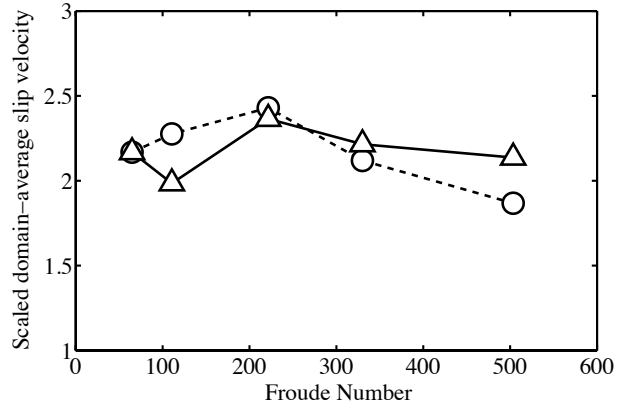

Figure 3: Scaled slip velocity at different Froude numbers: Triangles: L_I scaling; Circles: L_{II} scaling.

We then examined how one should scale the filter size for other Froude number values so that appropriately scaled filtered quantities were essentially the same for all Froude numbers. In view of results presented in Figure 2, we allowed the grid resolution to scale with n = -2/3 (so that in all the cases we were resolving the flow field on a length scale given by the competition between gravity and the particle phase deviatoric stress arising through particle-particle interactions). Figure 3 shows the scaled slip velocity for different Froude numbers. The triangles and circles were obtained when the filter size was scaled using $L_I = u_t^2 / g$ and $L_{II} = \left(u_t^2 / g \right) Fr_p^{-2/3}$, respectively. Although both scaling yield nearly the same results, the inertial scaling appears to be slightly superior for the larger particles; for the smaller particles, the trend is somewhat erratic for both scaling, and this could be due to grid independence being more difficult to achieve for smaller particles. Comparing this with the results presented in Figure 2, it seems reasonable to infer the following: (a) while the n = -2/3 is distinctly superior to n = 0 scaling for small filter sizes, they become comparable for larger filter sizes; or, (b) while the n = -2/3 is distinctly

superior to n = 0 scaling for small filter sizes, the n = 0 scaling becomes more appropriate for larger filter sizes (i.e., as filter size increases, the exponent shifts from -2/3 towards 0). At the present time, it is not possible to discriminate between these two hypotheses.

For the base case system, which has been studied in detail in the literature ([11]), the fluctuations arising from the clusters and streamers contribute much more to the filtered viscosity of the particle phase, when the filter size, Δ_f = 0.5 cm or larger; these fluctuations are associated with the inertial terms on the left hand side of eq. (2), and the particle phase stress associated with fluctuations at the scale of the individual particles (captured by σ_s in eq. 2) contribute negligibly. Thus, inertial scaling L_I does appear to be the most meaningful scale for filter size larger than ~0.5 cm for the base case.

Filtered viscosity scaling can be examined in several different ways:

a) As mentioned earlier, the rate of dissipation of mechanical energy per unit volume in our test example scales as $\rho_s \langle \phi_s \rangle u_t g$; if one adapts the typical scaling analysis of single-phase turbulent flow $\rho_s \langle \phi_s \rangle u_t g \sim \rho_s \langle \phi_s \rangle u_f^3 / \Delta_f$ where u_f is the average fluctuation velocity at the filter scale. So, $u_f \sim \left(g u_t \Delta_f \right)^{1/3}$; and, the filtered particle phase viscosity $\mu_{f,s} \sim \rho_s u_f \Delta_f \sim \rho_s \left(g u_t \Delta_f \right)^{1/3} \Delta_f$.

b) A simpler scaling argument would assert that the fluctuating velocity scales as the terminal velocity and so $\mu_{f,s} \sim \rho_s u_f \Delta_f \sim \rho_s u_t \Delta_f$.

Indeed, the filter size dependence observed for the 75 micron particles in earlier studies ([12]), namely ~1.2, is in between these two estimates.

Our recent study shows that the filtered dispersion coefficients for momentum, species and energy in both gas and particle phases ([2]) $\sim \Delta_f^2 S$ where S is the filtered scalar shear rate. This is exactly the same scaling as in the Smagorinsky model for sub-grid dispersion in single-phase turbulence ([13]), which further supports the inertial origin for the dispersion arising from sub-filter scale processes. This $\Delta_f^2 S$ scaling does away with a need to identify reference length scale for the dispersion coefficients.

DISCUSSION

The physical implication of the results presented above is as follows. Fine structure (typically on a scale of tens of particle diameters) seen in gas-particle flow is set by the competition between gravitational stress and deviatoric stress in the particle phase (attributable to streaming, collisional and frictional interactions, and captured by the kinetic theory of granular materials). On a coarser scale (several hundred

particle diameters), the meso-scale fluctuations play a much larger role. The relevant length scales for coarse and fine structures are L_I and L_{II}, respectively.

Results gathered in this study and in the literature suggest that the dispersion coefficients for momentum, species and energy for the particle and fluid phases in filtered two-fluid models for gas-particle flows is a consequence of sub-filter scale velocity fluctuations, and so inertial scaling is suggested for these quantities.

CONCLUSION

The friction coefficient to be used in coarse-grid simulations of gas-particle flows will, in general, be different from the microscopic friction coefficients commonly used for nearly homogeneous suspensions. Specifically, the sub-filter scale inhomogeneities will lower the effective friction coefficient. How to scale the filter size appearing in the model for this reduction in the friction coefficient remains an unresolved question. Our CFD-DEM simulations suggest that when the filter size is only on the order of a few tens of particle diameters, it is best scaled using a characteristic length obtained by balancing particle phase deviatoric stress and gravitational stress. With much larger filter sizes, proper choice of characteristic length is less clear; it seems likely that the characteristic length gradually shifts to one defined by the balance of inertial and gravitational stresses. It should be noted that at sufficiently large filter sizes the correction to the friction coefficient appears to become independent of filter size (e.g., see ref. 12,14); so, this difference may not be critical in simulation of flows in large process vessels using filtered models, where one would essentially be using the large-filter-size asymptote for the friction coefficient.

NOTATION

d	particle diameter [m]
Fr_p	Particle Froude number
g	gravitational acceleration [m/s²]
$L_I - L_V$	various reference lengths [m]
L_f	reference length to scale the filter lengths [m]
p_g	gas pressure [Pa]
T	granular temperature [m²/s²]
u_f	fluctuating velocity at filter scale [m/s]
u_s	gas-particle slip velocity [m/s]
u_t	terminal settling velocity [m/s]
$v_g ; v_s$	velocity (gas; particle) [m/s]

V_{slip} domain-average gas-solid slip velocity [m/s]

Greek Symbols

$\Delta_d; \Delta_f$ length (domain; filter) [m]

$\rho_s; \rho_g$ density (particle; fluid) [kg/m³]

$\phi_s; \phi_g$ volume fraction (particle; fluid)

μ_s, μ_g viscosity (particle; fluid) [Pa.s]

$\mu_{f,s}$ filtered particle phase viscosity [Pa.s]

$\sigma_s; \sigma_g$ stress (particle; fluid) [Pa]

REFERENCES

[1]   C. C. Milioli, F. E. Milioli, W. Holloway, K. Agrawal and S. Sundaresan, Filtered two-fluid models of fluidized gas-particle flows: new constitutive relations. Submitted to *AIChE J.* (2012).

[2]   K. Agrawal, W. Holloway, C. C. Milioli, F. E. Milioli and S. Sundaresan, Filtered models for scalar transport in gas-particle flows. Submitted to *Chem. Eng. Sci.* (2012).

[3]   L. R. Glicksman, Scaling relationships for fluidized beds. *Chem. Eng. Sci.,* 39 (1984) 1373-1379.

[4]   L. R. Glicksman, M. Hyre and K. Woloshun, Simplified scaling relations for fluidized beds. *Powder Technol.,* 77 (1993) 177-199.

[5]   B. Leckner, P. Szentannai and F. Winter. Scale-up of fluidized bed combustion – a review. *Fuel,* 90 (2011) 2951-2964.

[6]   C. Wen and Y. Yu, Mechanics of fluidization. Chem. Eng. Prog. Symp. Ser., 62 (1966) 100–111.

[7]   K. Agrawal, P. N. Loezos, M. Syamlal and S. Sundaresan. The Role of meso-scale structures in rapid gas-solid flows. *J. Fluid Mech.*, 445 (2001) 151-185.

[8]   D. Gidaspow. *Multiphase Flow and Fluidization*, Academic Press, CA. 1994.

[9]   H. P. ZHU, Z. Y. Zhou, R. Y. Yang and A. B. Yu. Discrete particle simulation of particulate systems: A review of major applications and findings. *Chem. Eng. Sci.*, 63 (2008) 5728-5770.

[10]   M. Syamlal, W. Rogers and T. O'Brien. *MFIX Documentation*. Morgantown, WV: U.S. Department of Energy, Federal Energy Technology Center, 1993.

[11]   Y. Igci, A. T. Andrews, S. Pannala, T. O'Briens and S. Sundaresan. Filtered two-fluid models for fluidized gas-particle suspensions. *AIChE J.*, 54 (2008) 1431-1448.

[12]   Y. Igci and S. Sundaresan. Constitutive models for filtered two-fluid models of fluidized gas-particle flows. *Ind. Eng. Chem. Res.,* 50 (2011) 13190-13201.

[13]   J. Smagorinsky. General circulation experiments with the primitive equations. *Monthly Weather Rev.*, 91 (1963) 99-164.

[14]   J.-F. Parmentier, O. Simonin and O. Delsart. A functional subgrid drift velocity model for filtered drag prediction in dense fluidized bed. *AIChE J.,* 58 (2012) 1084-1098.